The Spatial Distribution of Excitatory and Inhibitory Inputs to Ganglion Cell Dendrites in the Tiger Salamander Retina

Peter D. Lukasiewicz and Frank S. Werblin

Division of Neurobiology, Department of Cell and Molecular Biology, The University of California, Berkeley, California 94720

In response to focal stimuli, ganglion cell dendrites receive excitation over a relatively narrow extent of the inner plexiform layer (IPL). This excitation is embedded in 2 wider lateral inhibitory regions. Here we estimate the lateral dimensions of the inhibitory regions. Ganglion cells were whole-cell patch-clamped and dendrites were identified and located in retinal slices using Lucifer yellow in the pipettes.

The spatial distribution of ganglion cell dendritic sensitivity was measured with puffs of transmitter substances applied at different distances along the dendrites. All ganglion cell dendrites were sensitive to glutamate, GABA, and glycine across their full extent. The responses to puffs decreased with lateral distance from the soma and were well fit by Gaussians. The responses to puffs of potassium showed a similar decrement with distance. Since potassium channels are probably uniformly distributed along the dendrites, the similarity in profiles suggests that receptor density is also uniform along the dendrites.

The spatial distribution of responses of ganglion cells to excitatory and inhibitory synaptic inputs was measured by depolarizing local populations of bipolar terminals (and subsequently local populations of amacrine cells) with transretinal current (TRC). TRC-stimulating electrodes were displaced laterally, with respect to the ganglion cell soma, to generate response profiles.

We estimated the dimensions of the inhibitory and excitatory signals received by the ganglion cells by removing the contributions of their dendrites, the stimulus, and other interneurons from the response profiles. The excitatory signal extended less than 100 μm, the approximate dimensions of the ganglion cell dendrites, and corresponds roughly to the width of the bipolar inputs. The GABAergic signal extended, on average, 253 μm and glycinergic signal extended, on average, 315 μm. These inhibitory signal dimensions correspond to the width of classes of amacrine cell processes measured in other studies.

Ganglion cells receive a rich complement of direct excitatory and inhibitory synaptic inputs, suggesting that some forms of neural integration, including lateral interactions, may be mediated at the dendrites. In salamander, the excitatory inputs to all ganglion cell types are mediated primarily by glutamate (Slaughter and Miller, 1983; Lukasiewicz and McReynolds, 1985). ON and OFF ganglion cells also receive *sustained* inhibitory inputs at light OFF and ON, respectively (Belgum et al., 1982), and the sustained inhibitory input at light ON may be mediated by GABA (Belgum et al., 1984). In addition, all 3 types of ganglion cells receive *transient* inhibitory inputs at light ON and OFF (Wunk and Werblin, 1979) that are thought to be mediated by glycine (Belgum et al., 1984).

Although it is difficult to distinguish between antagonism at the inner and outer retina using light stimuli, some of the spatial characteristics of antagonistic receptive fields mediated at the inner plexiform layer (IPL) have been characterized. One type of lateral inhibitory pathway is driven by change in the surround (Werblin, 1972; Werblin and Copenhagen, 1974). A steady surround antagonism at the IPL has also been described (Belgum et al., 1987).

As a step toward identifying the cell types and clarifying the neural pathways underlying lateral antagonism at the IPL, we attempted here to define the spatial extent across the IPL, over which each transmitter substance would be released in response to a focal stimulus. We first probed the dendrites of identified ganglion cell types directly with each transmitter substance to determine their *sensitivity profiles*. Then we measured the *response profiles* to focal stimulation of the bipolar terminals to determine the lateral extent over which specific synaptic signals in the IPL impinged on these dendrites.

Our measurements suggest that excitatory signals are confined to a region not much broader than the dendrites of the ganglion cells. Inhibitory signals extend more broadly and may be mediated by GABAergic and glycinergic interneurons with processes distributed over a wider area of the IPL than the ganglion cell dendrites. Distinct morphological types of amacrine cells have been suggested to mediate GABAergic and glycinergic inputs at the IPL (Werblin et al., 1988). Here we show that the widths for the 2 inhibitory signals we measure in the IPL are similar to the process dimensions for chemically identified GABAergic and glycinergic amacrine cells (Yang et al., 1989).

Materials and Methods

Whole-cell patch recording in retinal slices. Details regarding the application of whole-cell patch recording (Hamill et al., 1981) in retinal slices (Werblin, 1978) have been described in detail elsewhere (Barnes and Werblin, 1986, 1987; Lukasiewicz and Werblin, 1988).

Puffing transmitter substances at the ganglion cell dendrites. Responses were elicited by "puffing" either glutamate (0.1–1 mM), kainate (10–50 μM), GABA (50–1000 μM), or glycine (50–500 μM) through pipette tips of ≤1-μm diameter onto ganglion cell dendrites. The tip was moved laterally along the dendrites to determine the spatial sensitivity of each

Received Mar. 27, 1989; revised June 19, 1989; accepted June 22, 1989.

This work was supported by NIH grant EY00561 (to F.W.) and NIH Postdoctoral Fellowship EY05751 (to P.L.). We thank Scott Eliasof, George Grant, and Dr. John McReynolds for their helpful comments on this work.

Correspondence should be addressed to Dr. Frank S. Werblin at the above address.

transmitter substance. Substances were pressure-ejected (2–15 psi for 20–75 msec) using a solenoid-controlled pneumatic valve. All puffing measurements were performed after synaptic transmission was blocked by replacing the calcium in the bathing medium with 1 mM Cd^{2+} and 3 mM Mg^{2+}. No desensitization was observed when substances were puffed repeatedly at 30-sec intervals, even when the pipette remained at the same location.

Puff calibration. The effective spread of the puffs was determined by puffing glutamate (1 mM), GABA (500 μM), or potassium (134 mM) in the presence of cadmium and magnesium, over a single isolated process of a ganglion cell in the slice. Figure 1*A* shows a series of responses elicited when potassium was puffed at increasing distances perpendicular to an isolated process. Maximum responses were elicited when the puff pipette was positioned directly over the process. Responses decreased in magnitude and increased in time to peak as the puff pipette was moved away from the process, probably owing to diffusion of the puff to the region of sensitivity. The spatial distribution of puff, measured by response to potassium, glutamate, and GABA, is shown in Figure 1*B*. Its effective range was approximately 25 μm.

Transretinal current stimulation. Release from bipolar cell terminals was elicited by passing current (0.05–0.2 mA for 1 msec) across the slice from the photoreceptors to the ganglion cells. Two insulated silver chloride electrodes, about 70 μm in diameter, were placed on either side of the slice, one electrode at the photoreceptors, the other at the ganglion cells. These electrodes were displaced laterally along the slice relative to the *recorded* ganglion cell to measure the spatial distribution of its synaptic inputs. No synaptic responses were elicited when current was passed in the opposite direction (i.e., from ganglion cells to photoreceptors).

Although photoreceptor terminals were probably also driven by the stimulus with respect to the ganglion cell responses reported here, photoreceptor transmitter release was most likely overwhelmed by the direct effect of the current on bipolar terminals. For example, excitatory responses were elicited in ON ganglion cells known to be driven by ON bipolar cells, yet photoreceptor transmitter release to ON bipolar dendrites would decrease transmitter release to ON ganglion cells. This suggests that photoreceptor transmitter release plays little or no role in the measurements described here. The bipolar activity elicited by transretinal current (TRC) is not, strictly speaking, physiological in that both ON and OFF bipolar cells are depolarized simultaneously. But the lateral spread of excitation in bipolar cells, the significant parameter in these studies, should be the same whether both ON and OFF pathways are stimulated separately or simultaneously.

Standard electrode and bathing solutions. The standard intracellular solution consisted of (in mM): cesium sulfate 73, cesium chloride 7, HEPES 4, EGTA 2, calcium chloride 0.317, magnesium chloride 1, adjusted to pH 7.5 with CsOH. To change the chloride equilibrium potential the Cl^- concentrations were modified as indicated in the Results section by changing the ratio of cesium sulfate to cesium chloride.

The bathing medium contained (in mM): sodium chloride 120, potassium chloride 2, calcium chloride 4, magnesium chloride 1, glucose 3, HEPES 5, adjusted to pH 7.8 with NaOH. Picrotoxin 50 μM or bicuculline (200 μM) and strychnine (≤15 μM) were added to the bathing medium to block GABA- and glycine-evoked activity.

Results

Morphological identification of cell types

A representative set of ganglion cells stained with Lucifer yellow (Stewart, 1978) is shown in Figure 2. We found 4 major cell types, distinguished by the ramification of their processes at different depths within the IPL (Famiglietti et al., 1977; Nelson et al., 1978).

Figure 2*A* shows a cell with processes that ramified in the outer half of the outer plexiform layer (OPL). This class of cell typically had either a single process or multiple processes leaving the cell body and extending to the outermost part of the IPL (sublamina A), where it branched into finer dendrites extending radially up to 280 μm (mean radius ± SD, 118 ± 54.5). Twenty-five stained cells conformed to this pattern. We tentatively identified these as OFF ganglion cells by reference to the criteria of Famiglietti et al. (1977).

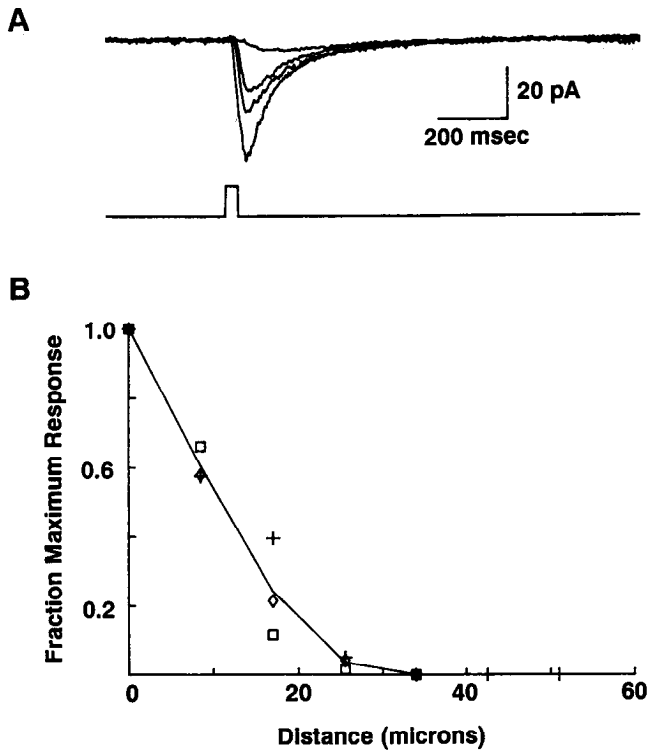

Figure 1. Spatial distribution of puffs of potassium, glutamate, and GABA. *A,* Responses to potassium puffed at an isolated process when the puff pipette was positioned 0, 8.5, 17, and 25.5 μm from the process. The largest amplitude response was at 0 μm, the smallest at 25.5 μm. In this and the following figures the trace below the responses indicates the time course of the gating of the puff pneumatic solenoid. *B,* Plot of the fraction maximum response vs puff pipette distance from an isolated process. The results from 3 different cells are shown when 134 mM potassium (*crosses*), 1 mM glutamate (*diamonds*), and 500 μM GABA (*squares*) were puffed. The *solid line* connects the average values at each distance.

Figure 2*B* shows a representative cell with processes that ramified in the inner half of the IPL (sublamina B). The processes extended radially by up to 255 μm (mean radius ± SD, 104.3 ± 40.4). We stained 40 cells with this morphology. These were tentatively identified as ON ganglion cells (Famiglietti et al., 1977; Nelson et al., 1978).

We found 2 distinct morphologies for (tentative) ON-OFF ganglion cells. Figure 2*C* shows 1 type with processes that were confined to the center region of the IPL ($n = 61$). The processes of this class extended radially up to 204 μm (mean radius ± SD, 104.5 ± 35.2). The other morphological type of ON-OFF ganglion cell is shown in Figure 2*D*. This cell's processes were multistratified, ramifying in *both* sublaminae a and b ($n = 81$). The processes of this class extended radially up to 221 μm (mean radius ± SD, 104.8 ± 36.3).

An axon was not clearly evident in every stained cell; some were probably lost during the slice procedure or not in the appropriate orientation for viewing. However, most cells in the ganglion cell layer appear to be ganglion cells, and not displaced amacrine cells, as shown by retrograde staining (Lukasiewicz and Werblin, 1988), so even cells without apparent axons in the ganglion cell layer are most likely ganglion cells.

For each of the 4 morphological types the response to steps of light or puffs of kainate at the OPL was consistent with its tentative functional identification (P. D. Lukasiewicz and F. S. Werblin, unpublished observations).

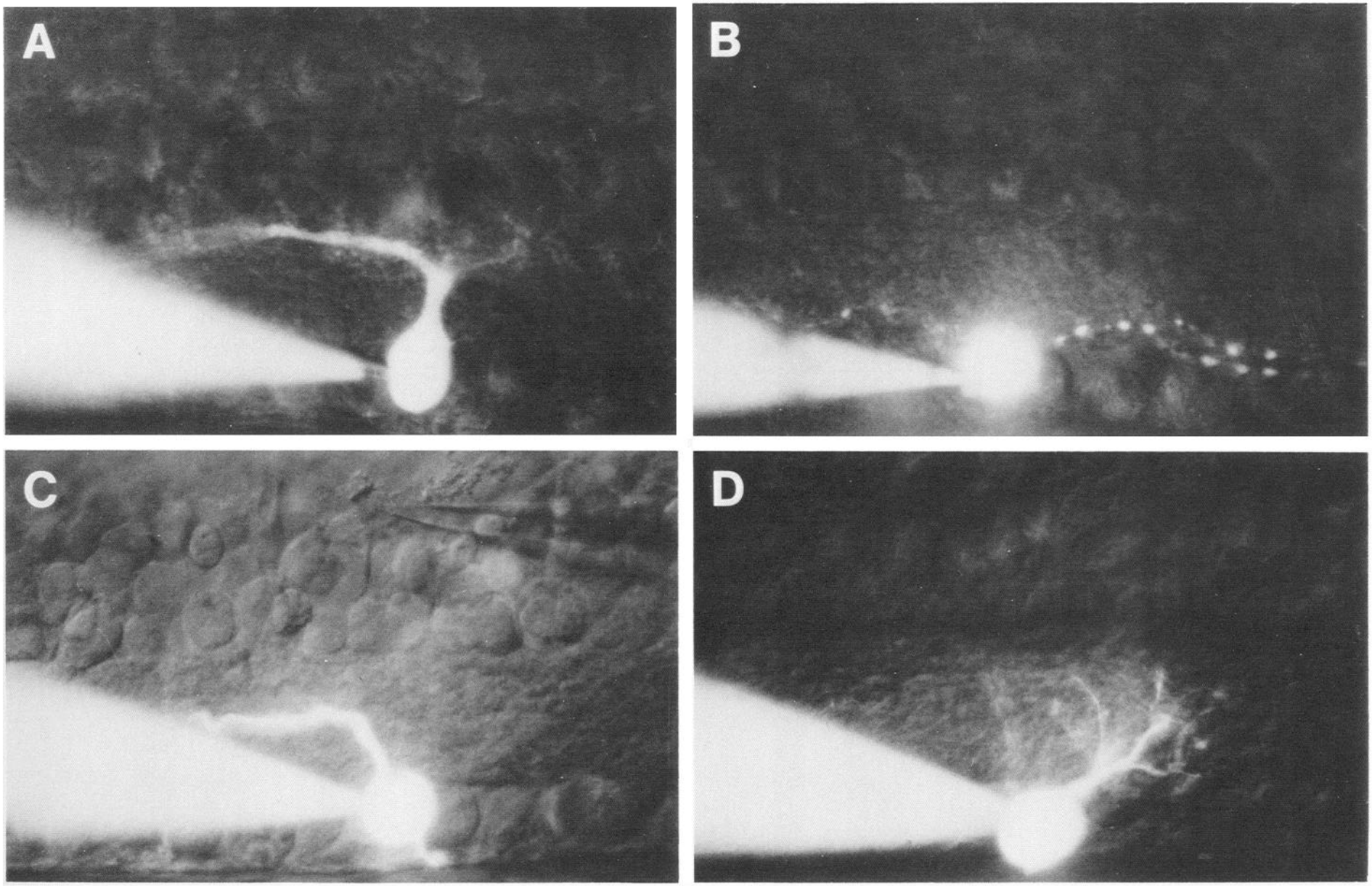

Figure 2. Photomicrographs of Lucifer yellow–filled ganglion cells (magnification, 750×). *A,* Ganglion cell with processes ramifying in the outer half of the IPL. This cell was most likely an OFF ganglion cell. *B,* Ganglion cell with processes ramifying in the inner half of the IPL, probably an ON cell. *C,* Ganglion cell with processes ramifying in the middle of the IPL, probably 1 kind of ON-OFF cell. *D,* Another ON-OFF ganglion cell morphology with processes ramifying throughout the IPL.

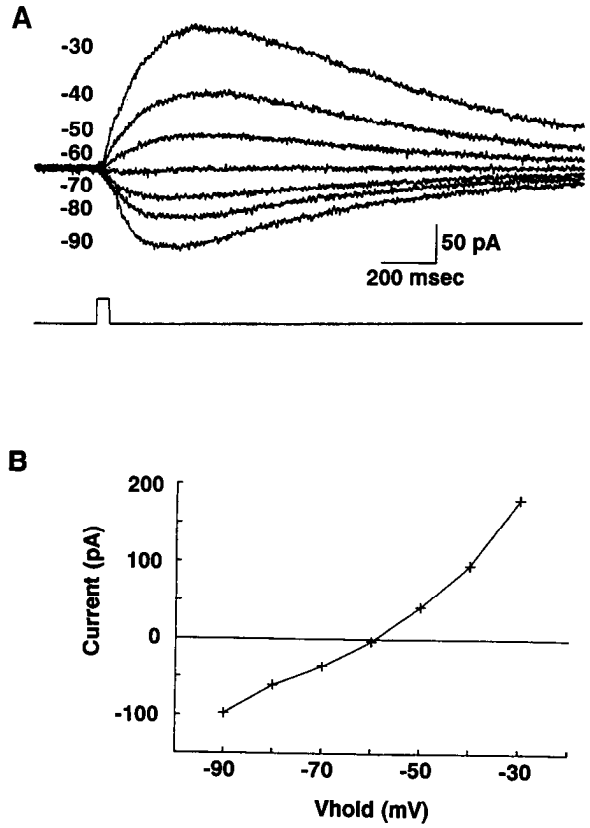

Figure 3. *A*, GABA-evoked currents in an OFF cell when the membrane was held at the potentials indicated at the left of each trace. Here and in the following figures the numbers correspond to the traces in descending order. GABA concentration in the pipette was 500 μm. Currents were leak-subtracted. *B*, Current-voltage relation for the GABA-elicited currents in *A*. E_{Cl} was set to -62 mV (pipette $[Cl^-]$ was 11.2 mM); the measured current reversed near -60 mV.

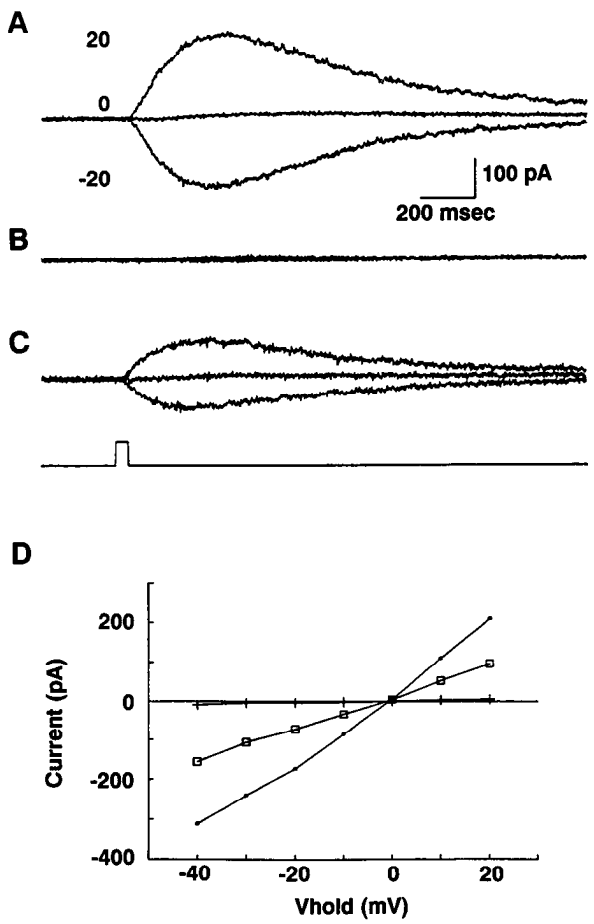

Figure 4. Reversible effects of picrotoxin on the GABA current in an ON-OFF cell. *A*, GABA-evoked current (500 μM in pipette) when membrane was held at the indicated potentials. Currents were leak-subtracted. E_{Cl} was set to -2 mV (pipette $[Cl^-]$ was 120 mM). *B*, Blockade of GABA-elicited current with 50 μm picrotoxin in the bath. Cell held at the same potentials as in *A*. *C*, Recovery after picrotoxin was removed from the bath. Cell was held at same potentials as in *A* and *B*. *D*, Current-voltage relations showing that the GABA responses reverse near 0 mV, E_{Cl}. Control responses, *dots*. Responses in picrotoxin, *crosses*. Responses after recovery from picrotoxin, *open squares*.

Current-voltage relations and pharmacological blockade of transmitter-elicited currents

In the following sections we puffed transmitter substances at the dendrites of each ganglion cell type and measured the elicited currents under voltage clamp, derived the current-voltage relations, and confirmed the pharmacological effects using specific antagonists. In all measurements with puffs, synaptic transmission was blocked by replacing Ca^{2+} in the bath by Cd^{2+} and Mg^{2+} (see Materials and Methods). Similar results were found for all 3 types of ganglion cells; examples using a single cell type for each pharmacological input are given below.

GABA-elicited currents. GABA elicited a synaptic current that reversed near E_{Cl} in all ganglion cell types. Responses from an OFF ganglion cell to puffs of GABA at different holding potentials are shown in Figure 3*A*. The responses reversed near -60 mV, close to the calculated reversal for chloride (E_{Cl}), -62 mV. The current-voltage relation for the GABA-evoked responses is shown in Figure 3*B*. The GABA-evoked current was not significantly voltage-dependent and was similar to GABA currents measured in other types of retinal neurons (Kaneko and Tachibana, 1986; Atwell et al., 1987).

The reversal of the GABA-evoked current was strongly dependent on intracellular chloride concentration (Bormann et al., 1987). When the pipette chloride concentration was increased to 120 mM, the calculated value of E_{Cl} was -2 mV, and the GABA-evoked currents, measured in an ON-OFF ganglion cell, reversed near 0 mV as shown in Figure 4*A–D*.

The GABA-elicited currents could be antagonized by bath-applied picrotoxin (50 μM) as shown in Figure 4*B*. Picrotoxin washed out very slowly and recovery was often incomplete (Fig. 4*C*). Complete current-voltage relations illustrating the action of picrotoxin are shown in Figure 4*D*. Bicuculline methiodide (200 μM) also antagonized the actions of applied GABA (not shown).

All 3 types of ganglion cells (4 OFF, 6 ON, and 12 ON-OFF) responded to GABA. No systematic differences were observed in the response magnitudes of the 3 ganglion cell types.

Glycine-elicited currents. Glycine, like GABA, elicited a current that reversed near E_{Cl} in all ganglion cell types. Responses from an ON-OFF ganglion cell to puffs of glycine at different holding potentials are shown in Figure 5*A*. The glycine-evoked currents reversed near -60 mV. The current-voltage relation for the glycine-evoked responses is shown in Figure 5*B*. This current did not show any significant voltage dependency and

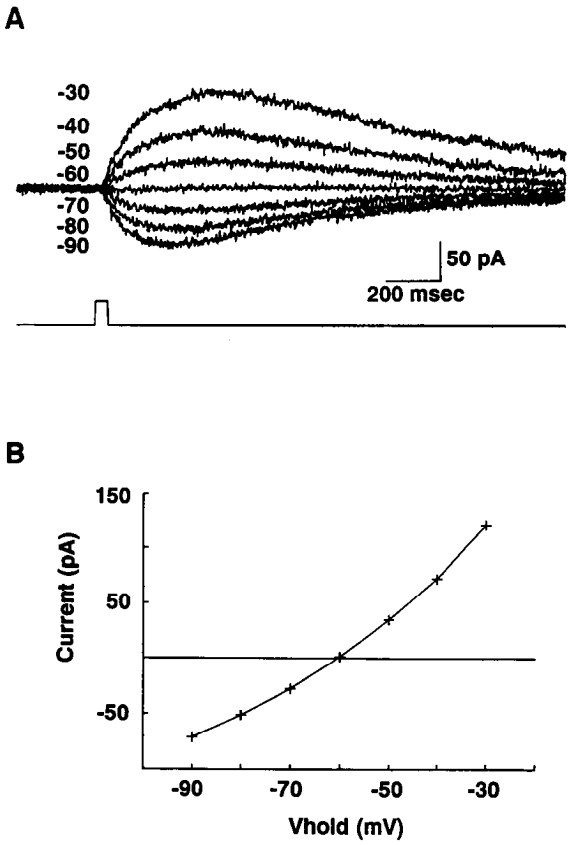

Figure 5. Glycine-evoked current in an ON-OFF cell. *A*, Responses to puffed glycine (500 μM in pipette). Membrane was held at the potentials indicated at the left of each trace. Currents were leak-subtracted. *B*, Current-voltage relation for the glycine-elicited currents in *A*. Currents reversed near −60 mV. E_{Cl} was set to −62 mV (pipette [Cl^-] was 11.2 mM).

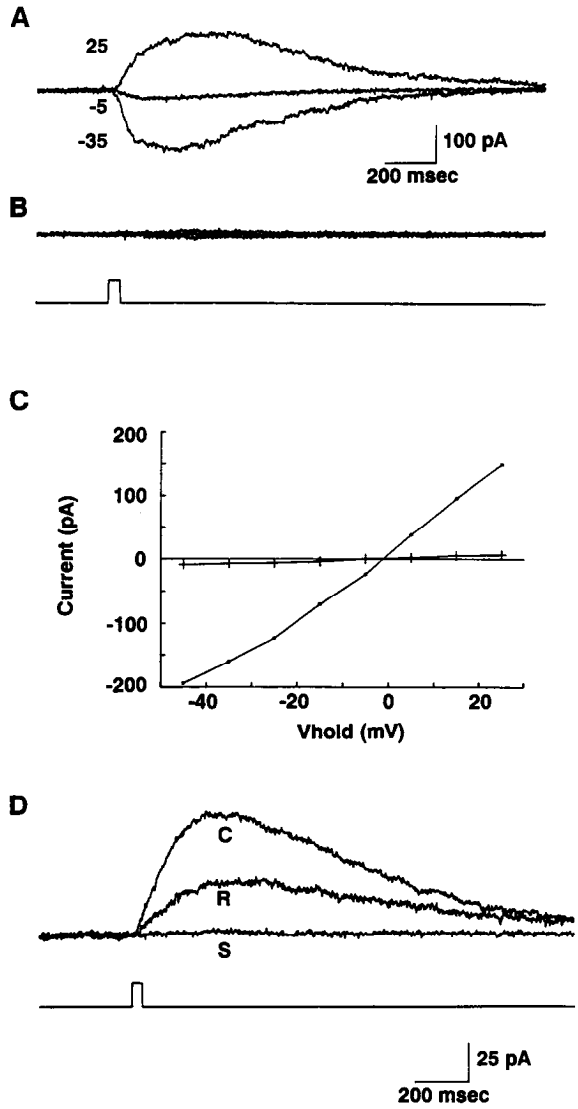

Figure 6. Reversible effects of strychnine on the glycine current in an ON-OFF cell. *A*, Glycine puff-evoked current (500 μM in pipette) when membrane was held at the indicated potentials. E_{Cl} was set to −2 mV (pipette [Cl^-] was 120 mM). *B*, Strychnine blockade (10 μm) of glycine current. Cell held at the same potentials as in *A*. The trace below the responses indicates the time course of the stimulus. *C*, Current-voltage relation showing that the glycine responses reverse near 0 mV. The control responses are shown as *dots*. The responses in the presence of strychnine are shown as *crosses*. *D*, Recovery of the glycine-evoked response (500 μM in pipette) from strychnine blockade shown in another cell (ON-OFF). The control trace is indicated by *C*, trace *S* was in the presence of 5 μM strychnine, and trace *R* shows recovery. The cell was held at −5 mV and E_{Cl} was set to −65 mV (pipette [Cl^-] was 9.6 mM).

reversed near the calculated reversal potential for chloride (−62 mV).

The reversal of the glycine-evoked current was strongly dependent on the chloride equilibrium potential (Barnes and Werblin, 1987; Bormann et al., 1987). Figure 6*A* shows a representative set of glycine-evoked currents from another ON-OFF cell in which the calculated E_{Cl} was −2 mV. The current-voltage relation for this ganglion cell is shown in Figure 6*C* with a reversal near −3 mV. Figure 6*B* shows the effects of bath-applied strychnine (10 μM) on the glycine-evoked response. The current-voltage relation illustrating the action of strychnine is shown in Figure 6*C*. Strychnine washed out slowly (>10 min), and cells were usually lost before recovery occurred. Partial recovery was found in only 3 cases; an example is shown in Figure 6*D*.

All 3 types of ganglion cells (1 OFF, 4 ON, and 9 ON-OFF) responded to glycine. No systematic differences were observed in the responses of the 3 ganglion cell types.

Glutamate and kainate-elicited currents. Both glutamate and kainate elicited inward currents over a physiological range of potentials for all ganglion cell types. The responses from an ON-OFF ganglion cell to puffs of glutamate are shown in Figure 7*A*. The glutamate-evoked currents reversed near 0 mV. Twenty cells responded to glutamate (6 OFF, 7 ON, and 7 ON-OFF) and no systematic differences were found.

The current-voltage relation for the glutamate-evoked responses is shown in Figure 7*B*. The current reversed near 0 mV, and the slope of the current-voltage curve decreased as the membrane was held at more negative potentials. This rectification is most likely due to the action of magnesium blocking glutamate-activated NMDA channels (Novak et al., 1984) on the ganglion cell (Slaughter and Miller, 1983; Lukasiewicz and McReynolds, 1985). The strength of the rectification varied from cell to cell, but no systematic differences were found among the different types of ganglion cells.

The responses of an OFF ganglion cell to puffs of kainate are shown in Figure 8*A*. The kainate-evoked currents also reversed near 0 mV. The current-voltage relationship for the kainate-

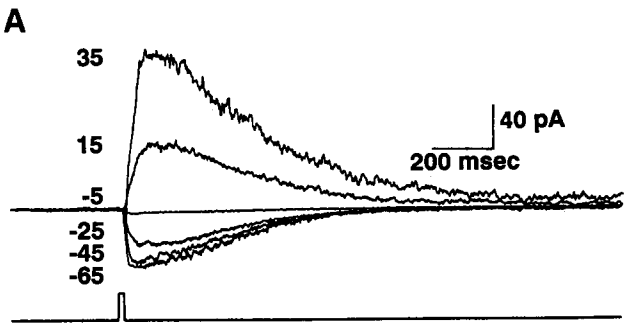

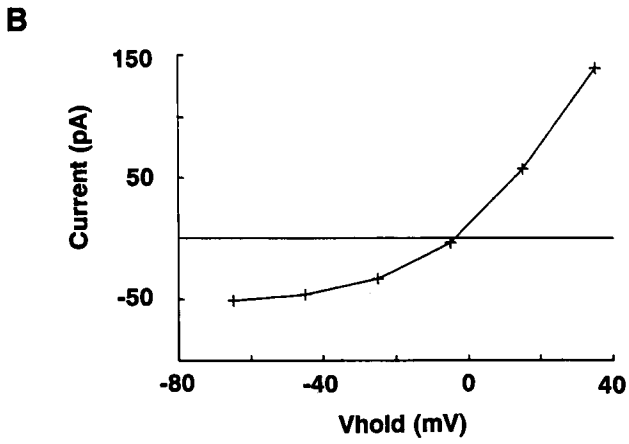

Figure 7. *A*, Glutamate-evoked currents (200 μM in pipette) in an ON-OFF cell when the membrane was held at the indicated potentials. E_{Cl} was set to −62 mV (pipette [Cl^-] was 11.2 mM). Currents were leak-subtracted. *B*, Current-voltage relationship for the glutamate-evoked current. The current reversed near 0 mV and rectified outwardly at negative potentials.

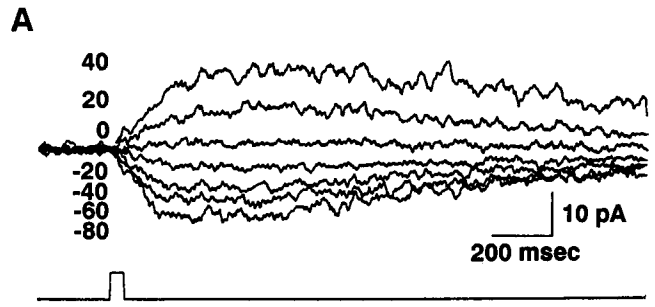

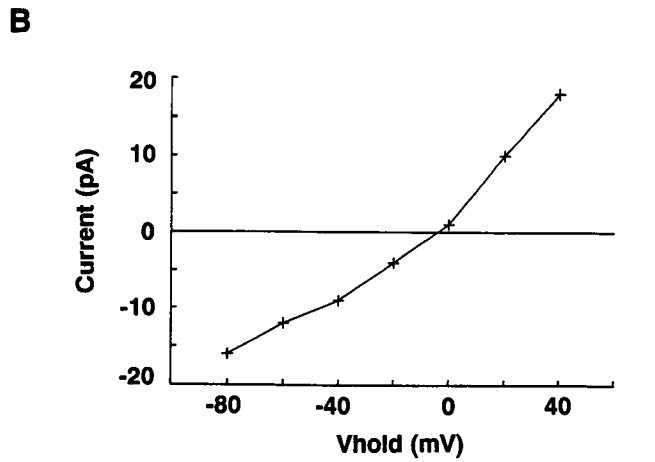

Figure 8. *A*, Kainate-evoked currents (10 μM in pipette) in an OFF cell when the membrane was held at the indicated potentials. E_{Cl} was set to −62 mV (pipette [Cl^-] was 11.2 mM). Currents were leak-subtracted. *B*, Current-voltage relationship for the kainate-evoked current. The current reversed near 0 mV and showed no significant rectification at negative potentials.

evoked responses are shown in Figure 8*B*. The kainate-evoked current showed no marked voltage dependence. All 8 cells tested (1 OFF, 3 ON, and 4 ON-OFF) responded similarly to kainate.

Dendritic spatial sensitivities as a function of lateral distance in the IPL

We measured the dendritic spatial sensitivities by first locating the processes of Lucifer-filled cells with brief epi-illumination. Transmitter substances were then puffed at different sites along the lateral extent of the processes.

Glutamate lateral sensitivity. The responses to applied glutamate, measured when the puff pipette was positioned at increasing lateral distances from the soma of an ON cell, are shown in Figure 9*A*. The responses, plotted as a function of lateral displacement, are shown in Figure 9*B*. This cell, like all others tested (4 ON-OFF, 2 OFF, and 4 ON), exhibited glutamate sensitivity over the full lateral extent of its dendritic processes.

The dendritic sensitivity profiles were fitted with a Gaussian function of the form

$$G(x) = \exp[-(x/L)^2] \quad (1)$$

where the value of L is a measure of the Gaussian "length constant," i.e., the displacement at which the function $G(x) = 1/e$. For the ON cell in Figure 9, the processes spanned a lateral distance of about 80 μm; the sensitivity profile was well fit by a Gaussian with an L-value of 63 μm.

GABA lateral sensitivity. The spatial sensitivity to GABA for an OFF cell is shown in Figure 10. Responses elicited at different puff pipette positions are shown in Figure 10*A*. This cell, like all others tested, showed GABA sensitivity (3 ON-OFF, 2 OFF, and 3 ON) over the full lateral extent of its dendritic processes. The normalized GABA-elicited responses are plotted as a function of puff pipette distance from the soma in Figure 10*B*. The measured lateral spread of the processes for this cell spanned 77 μm, and the GABA sensitivity profile was well fit with a Gaussian with an L-value of 59 μm.

Glycine lateral sensitivity. Responses to puffs of glycine for an ON cell are shown in Figure 11*A*. We measured glycine sensitivity across the full extent of the processes in all cells tested (3 ON, 5 ON-OFF, and 1 OFF). The measured lateral spread of the processes for this cell was 145 μm and the glycine sensitivity profile was well fit with a Gaussian curve having an L-value of 105 μm.

Spatial sensitivity to puffs of potassium. To determine whether the decrease in response with distance from the soma was due to a decrease in sensitivity (i.e., the number of receptors per unit area of membrane) or to a decrease in density of processes with uniform sensitivity (Freed and Sterling, 1989), we puffed

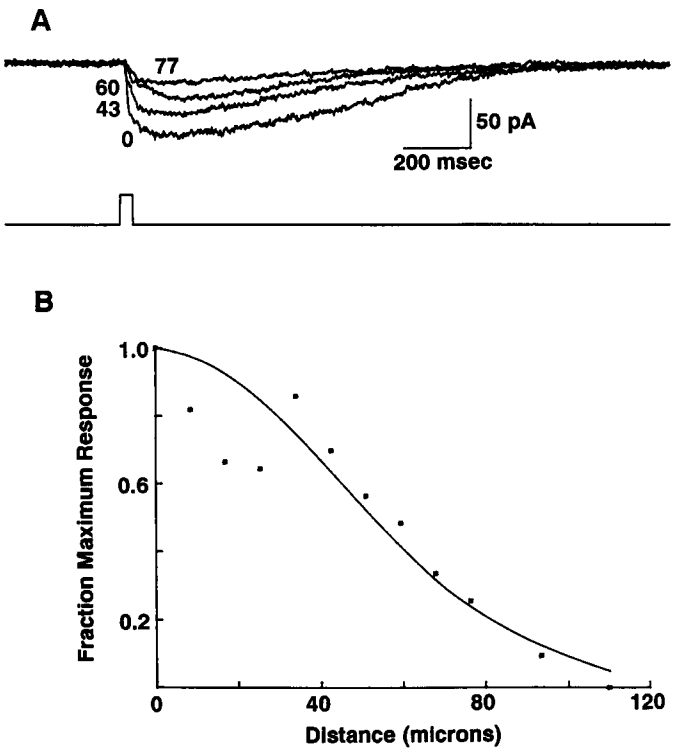

Figure 9. Lateral sensitivity to glutamate in an ON ganglion cell. *A*, Current responses to glutamate (1 mM) when the puff pipette was positioned at the indicated lateral distances from the soma. The membrane was held at −65 mV, E_{Cl} was set to −65 mV (pipette [Cl^-] was 9.6 mM). For all the lateral sensitivity experiments (also Figs. 10–12) cadmium (1 mM) and TTX (0.5 μM) were in the bath to block synaptic transmission and spiking. *B*, Plot of the responses shown as fraction maximal response vs lateral position of the puff pipette in the IPL. In this and the following figures the *solid line* is the best-fit Gaussian (see text).

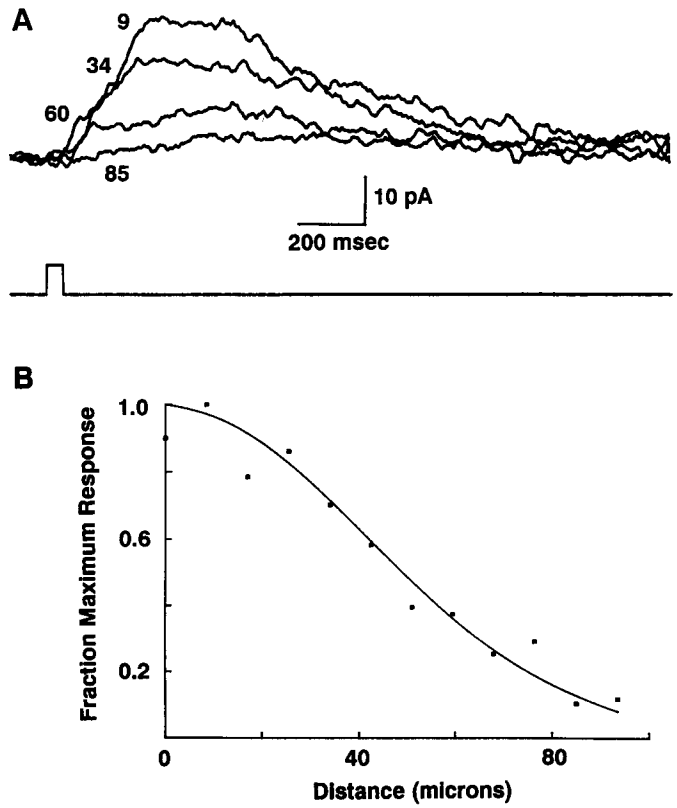

Figure 10. Lateral sensitivity to GABA in an OFF ganglion cell. *A*, Selected current responses to GABA (1 mM) when the puff pipette was positioned at the indicated lateral distances from the soma. The membrane was held at −22 mV, E_{Cl} was set to −65 mV (pipette [Cl^-] was 9.6 mM). *B*, Plot of the full complement of responses shown as fraction maximal response vs lateral position of the puff pipette in the IPL.

potassium along the processes and measured "potassium sensitivity" along the dendrites. The decrease in response was probably not due to electrotonic decay since ganglion cells have been shown to have high specific membrane resistances and long space constants (Coleman and Miller, 1989), which would result in only minimal attenuation of distally generated signals. Responses to the potassium puffs for an ON-OFF cell are shown in Figure 12*A*. The spatial sensitivity profile for potassium, plotted as a function of distance along the processes, is shown in Figure 12*B*. Potassium sensitivity extended along the full extent of the processes, with a profile decaying much like the sensitivities to the transmitter substances. Five cells tested with potassium showed similar results. The measured lateral extent of the processes was 68 μm, and the data were well fit by a Gaussian curve having an L-value of 49 μm.

Assuming the potassium channel density, as reflected by the specific membrane resistivity, is uniform along the dendrites (Gustafsson and Pinter, 1984), the finding that the potassium profile matches those of applied transmitters suggests that the decrease in response to transmitter measured along a cell's processes is probably due to a decrease in density of processes (Freed and Sterling, 1989). This suggests that the spatial sensitivities for GABA, glycine, and glutamate, measured along the lateral extent of the dendritic processes of ganglion cells, were uniform across the dendritic arbor.

The ratio of dendritic spread to Gaussian space constant is constant. The measured physical dimensions of the dendritic spread were variable from cell to cell. We generally selected cells whose processes were uniformly distributed laterally. For each cell the ratio of measured physical dendritic radius to the L-value, the exponent for the Gaussian best fit of the lateral sensitivity curves [see Eq. (1)] was constant. This ratio was 0.72 ± 0.04 (mean ± SD, $n = 18$). The consistency of this ratio, independent of the physical dimension of the dendrites, provides a way to estimate the radius of a dendritic field when only the L-value is known.

Although *all* cells showed sensitivity over the full extent of their dendritic fields, in some cells (44%) the measurements were erratic and not well fit by Gaussians. This was probably due either to obstructions at the slice (or pipette tip) or to variations in the depth, density, or distribution of the cell's processes.

The spatial distribution of responses elicited by TRC stimulation

Our aim here was to determine the response profiles for synaptically driven excitatory and inhibitory inputs to the ganglion cell. We elicited transmitter release from bipolar cell terminals with TRC (Toyoda and Fujimoto, 1984; Barnes and Werblin, 1987) as described in Materials and Methods. Unlike the puff responses above, these measurements were made without cadmium in the bath allowing the full complement of normal inputs from bipolar and amacrine cells to ganglion cells to be elicited. The ganglion cell was utilized as a sensor of transmitter release

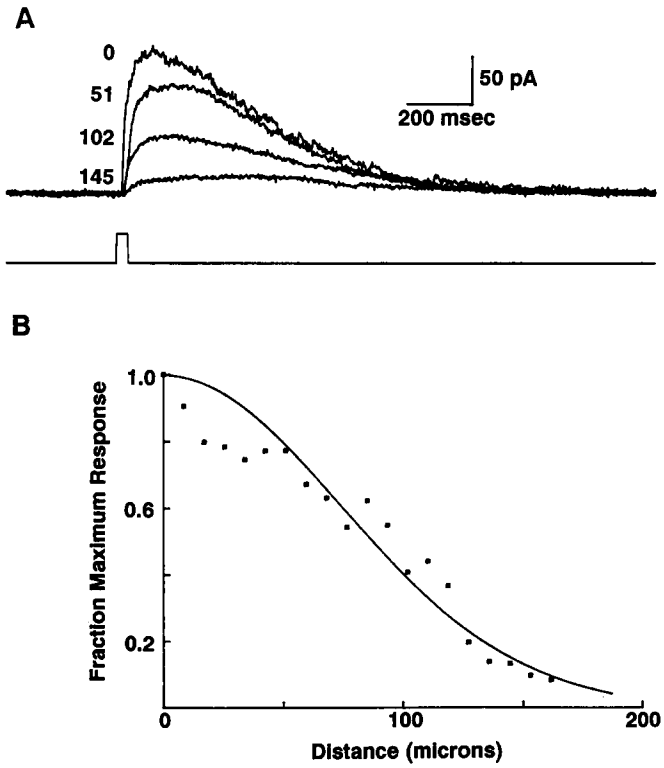

Figure 11. Lateral sensitivity to glycine in an ON ganglion cell. *A*, Selected current responses to glycine (200 μM) when the puff pipette was positioned at the indicated lateral distances from the soma. The membrane was held at −25 mV, E_{Cl} was set to −65 mV (pipette $[Cl^-]$ was 9.6 mM). *B*, Plot of the full complement of responses shown as fraction maximal response vs lateral position of the puff pipette in the IPL.

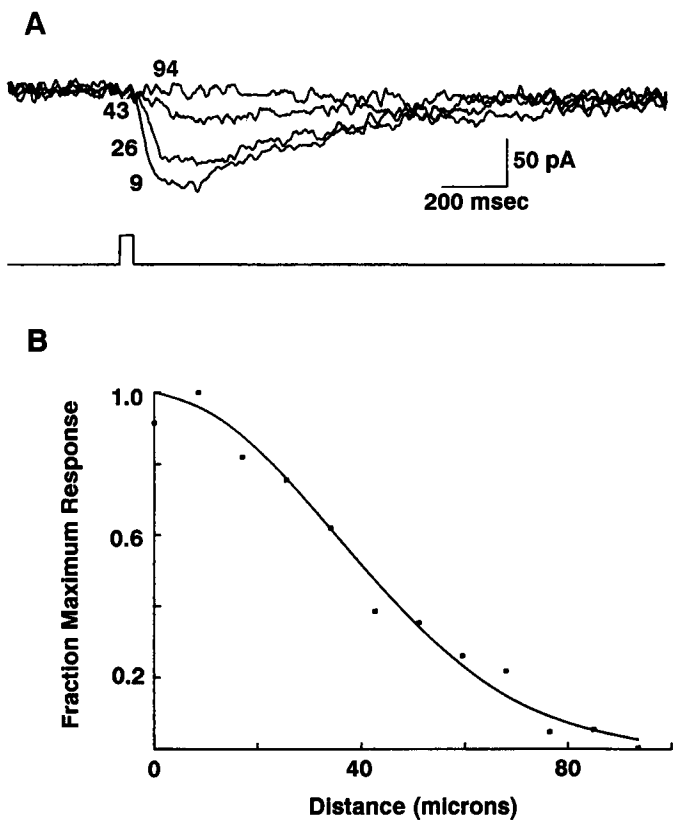

Figure 12. Lateral sensitivity to puffs of potassium (134 mM) in an ON-OFF ganglion cell. *A*, Selected current responses to potassium when the puff pipette was positioned at the indicated lateral distances from the soma. The membrane was held at −65 mV (pipette $[Cl^-]$ was 9.6 mM). Potassium sulfate/potassium chloride was substituted for cesium sulfate/cesium chloride in the pipette. *B*, Plot of the full complement of responses shown as fraction maximal response vs lateral position of the puff pipette in the IPL.

in the IPL. No systematic differences were found for different types of ganglion cells (7 ON-OFF, 4 ON, and 1 OFF) with respect to the experiments described below.

Response profile for excitatory input to ganglion cells. Excitatory inputs were isolated by holding the membrane at the reversal potential for the GABA and glycine inputs, near E_{Cl}. The stimulus pathway for eliciting bipolar transmitter release is shown schematically in Figure 13*A*.

The mean excitatory response profile from 4 ganglion cells when TRC was applied at different locations lateral to the cell body is shown in Figure 13*A*. The average of the measured lateral spread for the excitatory synaptic inputs was fitted with a Gaussian [see Eq. (1)] having an L-value of 120 μm ± 17 (mean ± SD). The average measured radius of the dendritic processes from these 4 ganglion cells was 133 μm ± 28 (mean ± SD).

Response profile for GABA-mediated inputs to ganglion cells. The GABA-mediated inhibitory inputs to ganglion cells were isolated by blocking the glycinergic inputs with strychnine while holding the membrane at 0 mV, the reversal potential for the excitatory input. The schematic in Figure 13*B* shows the stimulus pathway for eliciting the GABAergic inputs.

Figure 13*B* shows the magnitude of responses to GABA inputs as a function of stimulus displacement. A plot of the Gaussian best fit for the average responses of 6 cells is indicated by the solid curve. The L-value for the Gaussian was 216 μm ± 69 (mean ± 69 SD) for the GABA inputs. The mean dendritic radius for these 6 cells was 128 μm ± 44 (mean ± SD).

Response profile for glycine-mediated inputs to ganglion cells. The glycine-mediated inhibitory inputs to ganglion cells were isolated by blocking the GABAergic inputs with picrotoxin while holding the membrane at 0 mV, the reversal potential for the excitatory input. The schematic diagram in Figure 13*C* indicates the stimulus pathway for eliciting the glycinergic inputs.

The mean response profile for the glycine-mediated input as a function of stimulus position for 4 cells is shown in Figure 13*C*. These data were best fit by a Gaussian with an L-value of 258 μm ± 68 (mean ± SD). The mean dendritic radius for these 4 cells was 142 μm ± 25 (mean ± SD).

These measurements define the mean L-values for the Gaussian curves for the responses to excitatory, GABA-, and glycine-mediated inputs impinging on the ganglion cells. The pathway from stimulus to ganglion cell response includes the elements shown in Figure 13. In the Discussion we remove, by deconvolution, the contribution of the stimulus, bipolar, and ganglion cell dendrite spreads to derive the Gaussian curves describing the lateral distribution of the inhibitory signals across the IPL.

Discussion

Our results suggest that focal stimuli elicit activity within a relatively narrow excitatory zone, mediated by direct input from bipolar cells. This excitation is embedded in 2 separate, wider inhibitory regions, formed by GABAergic and glycinergic signals

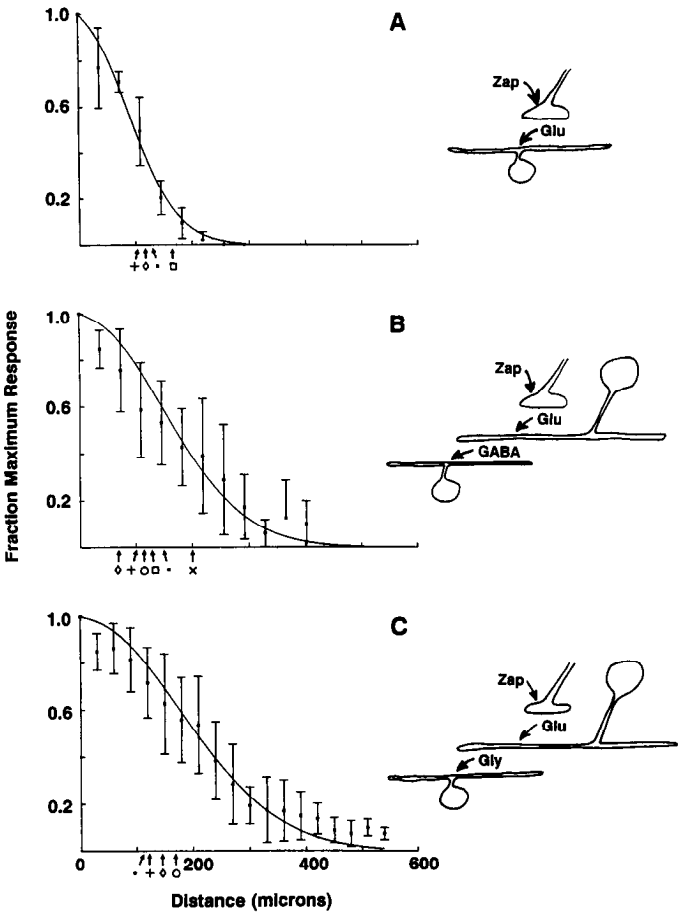

Figure 13. The spatial distribution of responses elicited by transretinal current. Normalized responses are plotted vs lateral position of the transretinal current electrodes aligned relative to the cell body of the recorded cell. *A, left,* Response profile for excitatory synaptic inputs from 4 different ganglion cells. In this and the following figures the *solid line* is the best-fit Gaussian of the average responses at each displacement, the *points* are the mean values, and the *bars* indicate the standard deviations. The dendritic radii for the measured cells were (in μm): 133 (*dots*), 171 (*open squares*), 106 (*crosses*), and 122 (*diamonds*) and are indicated by the *arrows* in this and the following figures. The cells were held at E_{Cl} (−65 mV), the reversal potential for GABA- and glycine-elicited responses. *Right,* Schematic of stimulus pathway. The *Zap* (TRC) evokes glutamate release from a population of bipolar processes which is sensed by the recorded ganglion cell. *B, left,* Response profile for GABA-mediated inhibitory synaptic inputs from 6 different cells. The dendritic radii (in μm) were 150 (*dots*), 102 (*crosses*), 115 (*open circles*), 130 (*open squares*), 200 (*Xs*), and 70 (*diamonds*). Strychnine (5 μM) was present in the bath to block glycinergic inputs. *Right,* Schematic of stimulus pathway. The *Zap* (TRC) excites a population of bipolar processes, which in turn evoke the release of GABA from a population of (presumed) amacrine processes which is sensed by the recorded ganglion cell. *C,* Response profile for glycine-mediated inhibitory synaptic inputs from 4 different cells. The dendritic radii (in μm) were approximately 125 (*crosses*), 150 (*diamonds*), 175 (*circles*), and 120 (*dots*). Picrotoxin (50 μM) was present in the bath to block the GABAergic inputs. *Right,* Schematic of stimulus pathway. The *Zap* (TRC) excites a population of bipolar processes, which in turn evoke the release of glycine from a population of (presumed) amacrine processes which is sensed by the recorded ganglion cell. For both *B* and *C* the cells were held at 0 mV, the reversal potential for the excitatory current, and E_{Cl} was set to −65 mV (pipette $[Cl^-]$ was 9.6 mM). Table 1 summarizes the response profiles for individual cells.

most likely mediated by amacrine cells. In the following, our estimates of the dimensions of the lateral spread of these 2 inhibitory signals suggest that they are carried by interneurons with process dimensions similar to the measured widths of some identified amacrine cells.

Uniform spatial sensitivity of ganglion cell dendrites

The dendrites of all morphological ganglion cell types are sensitive to the 3 major transmitter substances, glutamate, GABA, and glycine, previously reported to exist at the IPL (Miller et al., 1981; Slaughter and Miller, 1983; Belgum et al., 1984; Lukasiewicz and McReynolds, 1985). Moreover, the spatial sensitivity across the dendrites appears to be quite uniform. The spatial profiles for responses to puffs of these transmitters along the dendrites closely resemble the profile for potassium. Since potassium channels are probably uniformly distributed along the dendrites (see Results), we infer that all ganglion cell dendrites are uniformly sensitive to all 3 transmitter substances. We calculate below the lateral distribution of signals that normally impinge on the ganglion cell dendrites.

Deriving the spatial spread of excitatory and inhibitory signals received by ganglion cells.

A series of elements contributing to the spatial spread of the inhibitory response profile for the ganglion cells is shown in each synaptic pathway in Figure 13. The full lateral spread of the ganglion cell response profile is formed by the lateral spread of the stimulus, the spread of the bipolar cell terminals, the spread of the lateral inhibitory system, and the spread of the ganglion cell dendrites themselves. The spatial distribution for the lateral spread of the response profile and the spread of the dendrites has been measured. The lateral spread of the inhibitory signals can be calculated using deconvolution as described below.

The spatial profiles for ganglion cell sensitivity and those for the responses to excitatory and inhibitory synaptic inputs in the IPL were both well fit with Gaussian functions of the form of Eq. (1) repeated here:

$$G(x) = \exp[-(x/L)^2] \tag{1}$$

where L is a measure of the width of the Gaussian function, i.e., L is analogous to a space constant where $G(x) = 1/e$ when $x = L$. When a population of presynaptic elements with average Gaussian spatial spread $A(x) = \exp[-(x/a)^2]$ drives postsynaptic elements with spatial spread $B(x) = \exp[-(x/b)^2]$, the combined spread of the response, $C(x)$, measured in each postsynaptic element is given by the convolution of the two Gaussian functions $A(x)$ and $B(x)$. The Gaussian $C(x)$ resulting from the convolution has the form

$$C(x) = K \exp(-\{x/[(a^2 + b^2)^{1/2}]\}) \tag{2}$$

where K is given by

$$K = ab/(a^2 + b^2)^{1/2} \tag{3}$$

The space constant c for the combined Gaussian is

$$c = (a^2 + b^2)^{1/2} \tag{4}$$

Thus the width of any one of the 3 Gaussian functions can be easily computed, given the other 2. We use this method below to estimate each of the measured spatial spreads of the inhibitory system. The coefficient K is an index of the maximum amplitude of the function. We are concerned here only with the width of

the function, not its absolute amplitude. The width of the convolved function is independent of the relative amplitudes of the component Gaussians, so the value of K is not relevant.

The convolution integral is valid for linear signal transmission between populations of uniformly distributed neurons. The requirement for linearity is met in most cases since ganglion cells are thought to be isopotential, with space constants much wider than the processes (Coleman and Miller, 1989). So, under voltage clamp, excitatory or inhibitory inputs will probably sum linearly at the soma. Amacrine cells probably also sum their excitatory inputs from bipolar cells linearly. Like ganglion cells, amacrine cells have long length constants and may be close to isopotential (Eliasof et al., 1987). Furthermore, both amacrine and ganglion cells possess NMDA and non-NMDA receptors (Slaughter and Miller, 1983). The current-voltage curve for these excitatory channels is relatively flat in the physiological range (see Fig. 7), suggesting that under physiological conditions, each input acts as a current source without introducing a shunt and therefore sums linearly (Mittman et al., 1989).

Estimates of the widths of the excitatory inputs

Figure 13*A* shows the successive elements participating in the formation of ganglion cell excitatory input. The TRC (or Zap) drives an array of bipolar cell terminals that provide input to a ganglion cell. We can estimate the spread of the signal due to both TRC and the bipolar cells using Eq. (4).

The space constant L for the spread of the average excitatory response profile of the ganglion cells was 120 μm. This dimension includes the convolutions of spreads contributed by the TRC, the bipolar terminals, and the ganglion cell dendrites. The average ganglion cell dendritic radius for the 4 cells used in this measurement was 133 μm. We did not measure the spatial spread of sensitivity of the ganglion cells in Figure 13; however, we can predict the L-value for the sensitivity using the L-value to dendritic ratio of 0.72 derived in Results. This gives an estimate of the L-value for the average ganglion cell dendritic sensitivity as $0.72 \times 133\ \mu m = 96\ \mu m$. By deconvolving the ganglion cell dendrite contribution from the evoked excitatory spread using Eq. (4), we can estimate the TRC-bipolar cell contribution to be 72 μm (Fig. 14, curve B/T). This value of 72 μm is common to the TRC-bipolar component of the inhibitory responses as well, and we will use it below to derive the dimensions of the lateral inhibitory components by deconvolution.

Estimates of the spread of the GABA signal

The GABAergic response profile of the ganglion cells had an average L-value of 216 μm. This is the combined effect of the TRC, bipolar cells, inhibitory signal, and ganglion cell dendrites. All of these quantities are known except the spread of the inhibitory signal. Removing, by deconvolution, the mean ganglion cell dendritic spread (92 μm) and the spread of TRC-bipolar signal (72 μm) gives an estimate for the average L-value for the GABAergic inhibitory signal of 182 μm (Fig. 14, curve GAB).

Estimates of the spread of the glycinergic signal

By a similar process the glycinergic response profile of the ganglion cells was found to have an average L-value of 258 μm. When the spread of the mean ganglion cell field (100 μm) and the spread for the TRC-bipolar signal (72 μm) were removed using Eq. (4), the L-value for the glycinergic inhibitory signal was calculated to be 227 μm.

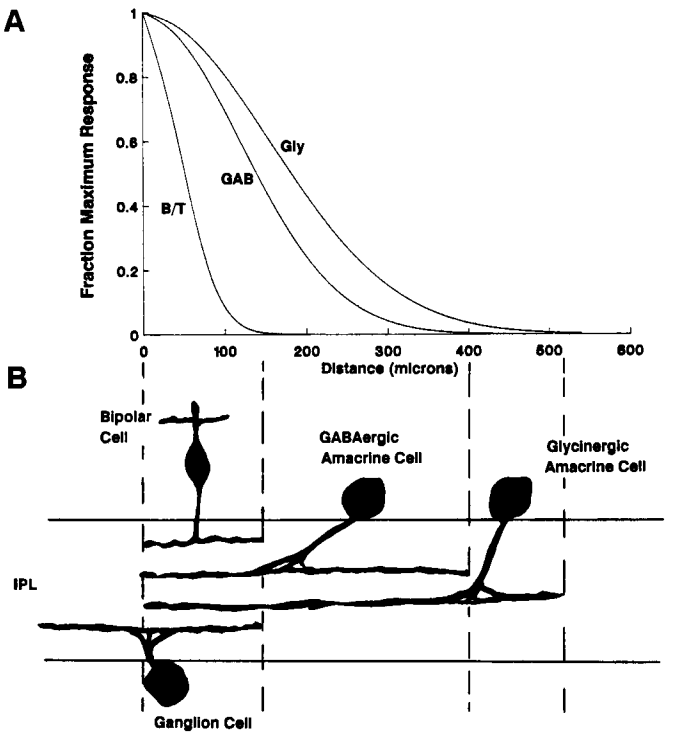

Figure 14. *A*, Lateral dimensions of the excitatory and inhibitory synaptic signals to ganglion cells estimated by deconvolution (see Discussion). *B/T* is the Gaussian derived for the average lateral spread for the TRC-bipolar combination. *GAB* is the Gaussian derived by deconvolution for the average GABAergic signal to the ganglion cell, and *Gly* is the Gaussian best fit for the average glycinergic signal to the ganglion cell. *B*, Sketches of the suggested amacrine cell types that fit the dimensions derived by deconvolution of the inhibitory signals and may provide the inhibitory inputs to a ganglion cell. The bipolar cell dimensions are overestimated because they include the spread of the stimulus, which cannot be measured independently.

GABAergic and glycinergic signals may be carried by specific classes of amacrine cells

Figure 14*A* shows the predicted Gaussian spreads for excitatory and inhibitory signals in the IPL. Sketches of likely neuronal sources of these signals are shown in Figure 14*B*. The excitatory signal, comprising the center of the receptive field, was, on average, about 100 μm wide, closely related to the radius of the ganglion cell dendrites, an idea originally proposed by Maturana et al. (1960). This suggests that the excitatory signal is not spread significantly further than the ganglion cell dendrites by a wide-field interneuron. Inhibitory signals impinge on the full extent of the dendritic field (the dendrites are uniformly sensitive to GABA and glycine, Figs. 9, 10). They appear to be carried from lateral distances *greater than* the spread of the ganglion cell dendrites, by populations of wide-field interneurons, most likely amacrine cells. The possibility that some wide-field signals may be mediated by electrically coupled amacrine cells (Naka and Christensen, 1981; Marc et al., 1988) of narrower dimensions cannot be ruled out.

The mean L-value for the GABAergic signal was 182 μm. The relationship between the L-values for the signal and the actual dimensions of the cells generating the signal is not known. But we can estimate the width of the cells using the ratio of L-value to dendritic spread derived here for *sensitivity* to estimate the *transmission* fields for the amacrine cells. Our L-value

Table 1. Dendritic sensitivity, response profile, and synaptic signal widths

Cell type	Dendritic radius	Dendritic sensitivity	Response profile width	Synaptic signal width
GABA-mediated inputs				
1 (ON-OFF)	150	108	174	116
2 (ON)	102	73	204	176
3 (ON-OFF)	115	83	318	299
4 (OFF)	130	94	276	250
5 (ON-OFF)	200	144	192	105
6 (ON-OFF)	70	50	130	96
			Mean ± SD	174 ± 84
Glycine-mediated inputs				
7 (ON)	120	86	182	143
8 (ON-OFF)	125	90	312	290
9 (ON-OFF)	150	108	218	175
10 (ON)	175	126	321	286
			Mean ± SD	224 ± 75
Excitatory inputs (+TRC)				
11 (ON-OFF)	133	95	100	31
12 (ON)	106	76	125	99
13 (ON-OFF)	122	88	131	97
14 (ON-OFF)	171	123	138	63
			Mean ± SD	72 ± 32

All values expressed in micrometers. Dendritic sensitivity, response profile width, and synaptic signal width are the L-values for the best Gaussian fits (see Discussion). The excitatory signals are overestimates since the spread of the stimulus (TRC) was not removed. The inhibitory synaptic signals were deconvolved using the mean excitatory signal width.

for the GABA-mediated signal of 182 μm predicts that the GABAergic amacrine cells would have processes that extend, on average, a radius of 253 μm as shown in Figure 14*B*.

Wide-field GABAergic amacrine cells may be the sources of the inhibitory inputs mediating steady center-surround antagonism at the inner retina (Belgum et al., 1987). Another class of GABA-mediated signals was relatively narrow (see Table 1). The latter class of signals may be mediated by relatively narrow-field GABAergic amacrine cells (Werblin et al., 1988) and may underlie the sustained inhibitory input evoked by central illumination in ganglion cells (Belgum et al., 1982, 1983), rather than acting as lateral interneurons.

Wide-field transient (or change-sensitive) inhibition to ganglion cells (Werblin, 1972; Werblin and Copenhagen, 1974; Wunk and Werblin, 1979) is believed to be mediated by glycinergic amacrine cells (Belgum et al., 1984) and is of similar dimension to the wide-field, glycinergic synaptic input (Maguire et al., 1989; Werblin et al., 1988) described here. The formula L-value/0.72 = dendritic radius predicts that the glycinergic amacrine cells span, on average, 315 μm.

Variations were found in the L-values for the inhibitory and excitatory signals as shown in Table 1. These variations were not correlated with cell type (e.g., ON vs ON-OFF) or the dimensions of the processes. Differences may be correlated with some other functional characteristic of the ganglion cell. In all cases the dimensions of the inhibitory signals were broader than those for the excitatory signals. The excitatory signal also includes the spread of the stimulus, so the actual dimensions for the excitatory signal were even narrower. The L-values of the GABA-mediated signals range from 96 to 299 μm and may reflect inputs dominated by relatively narrow-field or wide-field cells. A similar range of dimensions was found for immunohistochemically identified GABAergic amacrine cells (Yang et al., 1989). The L-values of the glycinergic signals ranged from moderate-field (143 μm) to wide-field (290 μm) and agree with the dimensions of immunohistochemically identified glycinergic amacrine cells (Yang et al., 1989).

From these studies we infer the lateral spread of pharmacologically specific *signals* across the IPL in response to a focal stimulus. We found average spreads of 253 μm for the GABAergic signal and 315 μm for the glycinergic signal. These dimensions are close to the measured dimensions of the cell *processes* of amacrine cells shown to be GABAergic and glycinergic (Yang et al., 1989). This suggests that the GABAergic and glycinergic amacrine cells are the sources of these inhibitory signals and that these cells generally are not coupled to form a syncytium, but probably act independently or are mutually inhibitory.

References

Atwell, D., P. Mobbs, M. Tessier-Lavigne, and M. Wilson (1987) Neurotransmitter-induced currents in retinal bipolar cells of the axolotl, *Ambystoma mexicanum*. J. Physiol. (Lond.) *387:* 125–161.

Barnes, S., and F. Werblin (1986) Gated currents generate single spike activity in amacrine cells of the tiger salamander retina. Proc. Natl. Acad. Sci. USA *83:* 1509–1512.

Barnes, S., and F. Werblin (1987) Direct excitatory and lateral inhibitory synaptic inputs to amacrine cells in the tiger salamander retina. Brain Res. *406:* 233–237.

Belgum, J. H., D. R. Dvorak, and J. S. McReynolds (1982) Sustained synaptic input to ganglion cells of mudpuppy retina. J. Physiol. (Lond.) *326:* 91–108.

Belgum, J. H., D. R. Dvorak, and J. S. McReynolds (1983) Sustained and transient synaptic inputs to on-off ganglion cells in the mudpuppy retina. J. Physiol. (Lond.) *340:* 599–610.

Belgum, J. H., D. R. Dvorak, and J. S. McReynolds (1984) Strychnine blocks transient but not sustained inhibition in mudpuppy retinal ganglion cells. J. Physiol. (Lond.) *354:* 273–286.

Belgum, J. H., D. R. Dvorak, J. S. McReynolds, and E.-I. Miyachi (1987) Push-pull effect of surround illumination excitatory and inhibitory inputs to mudpuppy retinal ganglion cells. J. Physiol. (Lond.) *388:* 233–244.

Bormann, J., O. P. Hamill, and B. Sakmann (1987) Mechanisms of anion permeation through channels gated by glycine and gamma-aminobutyric acid in mouse cultured spinal neurons. J. Physiol. (Lond.) *385:* 243–286.

Coleman, P. A., and R. F. Miller (1989) Measurement of passive membrane parameters with whole-cell recording from neurons in the intact amphibian retina. J. Neurophysiol. *61:* 218–230.

Eliasof, S., S. Barnes, and F. S. Werblin (1987) The interaction of ionic currents mediating single spike activity in retinal amacrine cells of the tiger salamander retina. J. Neurosci. *7:* 3512–3524.

Famiglietti, E. V., Jr., A. Kaneko, and M. Tachibana (1977) Neuronal architecture of ON and OFF pathways to ganglion cells in carp retina. Science *198:* 1267–1269.

Freed, M. A., and P. Sterling (1989) The distribution of synapses across the alpha ganglion cell arbor: Anatomical origin and physiological effect. Investig. Ophthal. Vis. Sci. *30* (Suppl.): 163.

Gustafsson, B., and M. J. Pinter (1984) Relations among passive electrical properties of lumbar α-motorneurons of the cat. J. Physiol. (Lond.) *356:* 401–431.

Hamill, O. P., A. Marty, E. Neher, B. Sakmann, and F. J. Sigworth (1981) Improved patch-clamp techniques for high resolution current recording from cells and cell-free membrane patches. Pflueger's Arch. *391:* 85–100.

Ikeda, H., and M. J. Sheardown (1982a) Aspartate may be an excitatory transmitter mediating visual excitation of "sustained" but not "transient" cells in the cat retina. Neuroscience *7:* 25–36.

Ikeda, H., and M. J. Sheardown (1982b) Acetylcholine may be an excitatory transmitter mediating visual excitation of "transient" cells

with the periphery effect in the cat retina: Iontophoretic studies *in vivo*. Neuroscience *7:* 1299–1308.

Kaneko, A., and M. Tachibana (1986) Effects of gamma-aminobutyric acid on isolated cone photoreceptors of the turtle retina. J. Physiol. (Lond.) *373:* 443–462.

Kirby, A. W., and C. Enroth-Cugell (1976) The involvement of gamma-aminobutyric acid in the organization of cat retinal ganglion cell receptive fields. A study with picrotoxin and bicuculline. J. Gen. Physiol. *68:* 465–484.

Lukasiewicz, P. D., and J. S. McReynolds (1985) Synaptic transmission at *N*-methyl-D-aspartate receptors in the proximal retina of the mudpuppy. J. Physiol. (Lond.) *367:* 99–115.

Lukasiewicz, P., and F. Werblin (1988) A slowly inactivating potassium current truncates spike activity in ganglion cells of the tiger salamander retina. J. Neurosci. *8:* 4470–4481.

Maguire, G., P. Lukasiewicz, and F. Werblin (1989) Amacrine cell interactions underlying the response to change in the tiger salamander retina. J. Neurosci. *9:* 726–735.

Marc, R. E., W. L. Liu, and J. F. Muller (1988) Gap junctions in the inner plexiform layer of the goldfish retina. Vision Res. *28:* 9–24.

Marchiafava, P. L., and V. Torre (1978) The responses of amacrine cells to light and intracellularly applied currents. J. Physiol. (Lond.) *276:* 83–102.

Maturana, H. R., J. Y. Lettvin, W. H. Pitts, and W. S. McCulloch (1960) Physiology and anatomy of vision in the frog. J. Gen. Physiol. *43* (Suppl.): 129–175.

Miller, R. F., T. E. Frumkes, M. M. Slaughter, and R. F. Dacheux (1981) Physiological and pharmacological basis of GABA and glycine action on neurons of mudpuppy retina. II. Amacrine and ganglion cells. J. Neurophysiol. *45:* 764–782.

Mittman, S., W. R. Taylor, and D. R. Copenhagen (1989) Characteristics of NMDA- and non-NMDA-receptor-mediated synaptic inputs to retinal ganglion cells. Investig. Ophthal. Vis. Sci. *30* (Suppl.): 162.

Naka, K.-I., and B. N. Christensen (1981) Direct electrical connections between transient amacrine cells in the catfish retina. Science *214:* 462–464.

Nelson, R., E. V. Famiglietti, and H. Kolb (1978) Intracellular staining reveals different levels of stratification for ON and OFF center ganglion cells in cat retina. J. Neurophysiol. *41:* 472–483.

Novak, L., P. Bregestovski, P. Ascher, A. Herbert, and A. Prochiantz (1984) Magnesium gates glutamate-activated channels in mouse central neurons. Nature *307:* 462–465.

Slaughter, M. M., and R. F. Miller (1983) The role of excitatory amino acid transmitters in the mudpuppy retina: An analysis with kainic acid and n-methyl aspartate. J. Neurosci. *3:* 1701–1711.

Stewart, W. W. (1978) Functional connections between cells as revealed by a highly fluorescent naphthalimide tracer. Cell *14:* 741–759.

Toyoda, J.-I., and M. Fujimoto (1984) Application of transretinal current stimulation for the study of bipolar-amacrine transmission. J. Gen. Physiol. *84:* 915–925.

Werblin, F. S. (1972) Lateral interactions at inner plexiform layer of a vertebrate retina: Antagonistic response to change. Science *175:* 1008–1010.

Werblin, F. S. (1978) Transmission along and between rods in the tiger salamander retina. J. Physiol. (Lond.) *280:* 449–470.

Werblin, F. S., and D. R. Copenhagen (1974) Control of retinal sensitivity. III. Lateral interactions at the inner plexiform layer. J. Gen. Physiol. *63:* 88–110.

Werblin, F., G. Maguire, P. Lukasiewicz, S. Eliasof, and S. Wu (1988) Neural interactions mediating the detection of motion in the retina of the tiger salamander. Visual Neurosci. *1:* 317–329.

Wunk, D. F., and F. S. Werblin (1979) Synaptic inputs to ganglion cells in the tiger salamander retina. J. Gen. Physiol. *73:* 265–286.

Yang, C. Y., P. Lukasiewicz, G. Maguire, F. Werblin, and S. Yazulla (1989) Neurochemical identification of lucifer yellow filled amacrine cells in tiger salamander retina. Investig. Ophthal. Vis. Sci. *30* (Suppl.): 119.